Low-energy elastic scattering of electrons from atomic oxygen



1989 J. Phys. B: At. Mol. Opt. Phys. 22 3529

(http://iopscience.iop.org/0953-4075/22/21/015)

J. Phys. B: At. Mol. Opt. Phys. **22** (1989) 3529-3539. Printed in the UK

# Low-energy elastic scattering of electrons from atomic oxygen

J F Williams† and L J Allen‡

† Department of Physics, The University of Western Australia, Nedlands, WA 6009, Australia

‡ School of Science and Mathematics Education, University of Melbourne, Parkville, VIC 3052, Australia

Received 26 April 1989, in final form 14 July 1989

**Abstract.** Electron scattering from atomic oxygen has been studied at energies from 0.5 to 8.7 eV. Absolute total (elastic plus inelastic) scattering cross sections have been measured by an attenuation method. Differential elastic cross sections from 10 to 150° have been measured with energy analysis of the scattered electrons. The apparatus uses crossed modulated electron and atomic beams with energy selection of the incident electron beam. Absolute cross section values have been determined from the measurement of experimental parameters using the relative gas flow method.

A parametrised phaseshift analysis has been made to determine phaseshifts from the measured elastic angular distributions. These 'elastic' phaseshifts are consistent within experimental accuracy with the calculations of Tambe and Henry and the variational calculations of Thomas and Nesbet. Integral elastic and momentum transfer cross sections were calculated from those phaseshifts. The measured total scattering cross section with an uncertainty of ±6% agrees with the polarised pseudostate calculations of Tambe and Henry but not with the Bethe-Goldstone calculations of Nesbet.

## 1. Introduction

This paper concerns the measurement of differential cross sections for elastic scattering, and the total scattering cross sections, of electrons from atomic oxygen. The relative elastic angular distributions are parametrised to determine the phaseshifts from which integral elastic and momentum transfer cross sections are evaluated. The main physical effects in the scattering process are direct and exchange scattering by the ground-state target, strong coupling effects with the low-lying excited states and polarisation of the target by the scattered electron. The long-range polarisation effects influence slow electrons more than fast electrons. Also s-wave electrons are more sensitive to short-range correlations than non-zero partial wave electrons since they have no centrifugal barrier. These physical effects have become well understood and the development of the theoretical methods generally has shown how to formulate them accurately.

There have been many theoretical considerations of elastic scattering from atomic oxygen but the reviews of LeDourneuf *et al* (1977) and Nesbet (1977, 1980) contain the essential features. In summary, both the polarised pseudostate and the Bethe-Goldstone approximations account for the main physical effects. The polarised pseudostate method has been developed from the polarised orbital method of Temkin (1957) and the close-coupling method of Seaton (1953). The pseudostates may be constructed to represent the first-order dipole perturbation of the core atomic wavefunction by an external electric field and the resulting coupled scattering equations solved

0953-4075/89/213529+11$02.50  

by direct integration (Tambe and Henry 1976) or by the $R$-matrix method (LeDourneuf *et al* 1977). The main alternative method is based on continuum Bethe-Goldstone equations. The collision wavefunction is expanded in a set of basis orbitals which are formulated to include the physical effects and which are expanded until convergence occurs. The solution of the Bethe-Goldstone equations is made using the matrix variational method. These two methods are generally considered to be satisfactory because they include the main physical effects and can explain at least elastic scattering from the simpler atomic gases. However they remain to be tested against experimental data for open-shell atoms such as atomic oxygen, nitrogen and carbon.

The only published measurement of elastic differential cross sections is by Dehmel *et al* (1976) for incident electron energies of 5 and 15 eV and scattering angles from 15° to 150°. The difficulty of such measurements is reflected by the absence of other publications and by the experimental limitations in the work of Dehmel *et al.* The formation of a reasonably dense atomic beam is difficult because a molecular dissociation method must be used. Their target beam was composed of 47% atoms with an unknown fraction in the ground state. The scattered electrons were detected without energy analysis so there are limitations to inferences that the measured signal arose predominantly from elastic scattering from ground state atoms. The earlier paper of Dehmel *et al* (1974), which determined the ratio of forward to backward scattered electrons, suffered from similar limitations.

The only measurement of total scattering cross sections is by Neynaber *et al* (1961) from 2.3 to 11.6 eV. Momentum transfer cross sections have been measured by Sunshine *et al* (1967) using the atomic beam recoil method from 0.5 to 11.3 eV, Lin and Kivel (1959) at 4000 K using a microwave absorption method and Daiber and Waldron (1966) using a shock tube method. These measurements were significant experimental achievements at their time. However they have such large experimental uncertainties that they are unable to indicate preference for any set of theoretical values.

## 2. Experiment

### *2.1. Apparatus*

The apparatus is a modulated crossed-beams type, with three differentially-pumped vacuum chambers to isolate the source and detector regions, which has been used in studies of electron scattering from atomic hydrogen (Williams 1988, Williams and Willis 1975). Those references give a complete description of the apparatus and method of measurement for the elastic differential cross sections. The principle of the measurement has not changed from that given initially by Boyd and Green (1958) and Brackmann *et al* (1958). A schematic arrangement of the present apparatus is given in figure 1. Molecular oxygen is partially dissociated in a discharge tube located in the first vacuum chamber. The beam is formed as the effusively emitted gas from the source passes through collimating apertures and an intermediate differential pumping chamber. Here the beam is mechanically chopped by a slotted rotating disc and it may be blocked by a shutter to assist with the identification of true beam and background signals. A 2 mm thin vacuum valve isolates this chamber from the scattering chamber so that the source and electron scattering apparatus can be maintained separately. The apparatus was designed to minimise the distance from the source to the interaction region but yet keep the atom beam chopper.

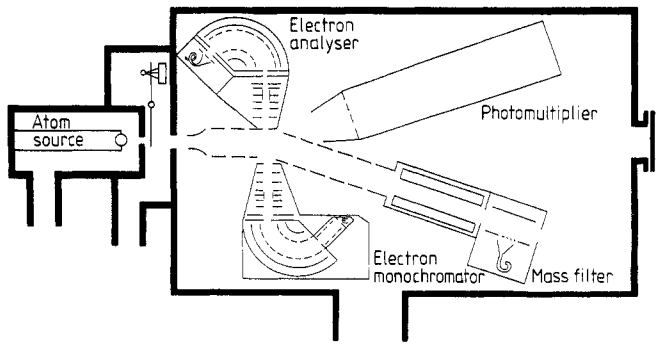


**Figure 1.** Schematic representation, not to scale, of the experimental apparatus.

The scattering chamber contains two 127° electrostatic electron energy selectors, one as a monochromator defining the incident electron beam and the other selecting the scattered electrons. Provision exists to mount another scattered electron analyser, a photon detector and a rotatable RF quadrupole for diagnostic purposes; the latter was used to determine the degree of dissociation of the oxygen beam as well as to study the scattered ion angular distribution. At the interaction region the characteristics of both beams were as follows. The incident electron beam had dimensions of $15 \times 1$ mm$^2$ with the 15 mm length parallel to the symmetry axis of the 127° monochromator and parallel to the axis of the atom beam. The electron beam angle was 0.5°, the pencil angle was 2° and for the present work the energy resolution was 0.25 eV. The oxygen beam was $3 \times 3$ mm$^2$ and entered the interaction region after passing through a small electric field to remove any ions from the discharge source and a 96% transparent grid to shield that field from the crossed-beams region. After the interaction region the gaseous beam entered a cylindrical electrostatic lens which focused ions into the RF mass filter. The photon detector consisted of collimating apertures to define an acceptance solid angle of $10^{-2}$ sr, a focusing lens to ensure parallel incident light on an interference filter of 2 nm width, linear and circular polarisers and an EMI 9588 photomultiplier tube.

Both beams were modulated. The electron beam was electrostatically deflected across a slit before the interaction region at a frequency of twice the mechanical chopping frequency of the neutral oxygen beam of 117.3 Hz. Each of the four resulting quadrants corresponded to the combinations of either beam on or off so that the interaction of the beams with one another and with the background could be measured. The scattered electron, photon or ion signals were recorded either in gated scalers or a multichannel analyser. The incident and scattered electron energy analysers could be electronically controlled so that either their pass energies or acceleration/deceleration lenses could be stepped through appropriate energy regions; however, in the present work this facility was used only for diagnostic purposes. At the low incident energies used for the present elastic scattering studies the analysers were tuned for a fixed pass energy. A Faraday cup measured the electron beam current entering a $15 \times 1$ mm$^2$ aperture as well as that falling onto a 1 mm wide region around the aperture. The ratio of current through the aperture to that outside the aperture was usually better than 100:1 at 8 eV. The incident electron current was about 1 $\mu$A at 8 eV, the oxygen beam density was about $10^7$ particles/cm$^3$ with an unknown velocity distribution, the detected elastically scattered electron count rate about 50 electrons/s into $10^{-2}$ sr.

The discharge source produced atomic and molecular ions and metastable atoms. The morphology of the operation of the source and its optimisation for a given output species is not pursued here other than to say that all parameters of the discharge affected the relative and absolute numbers of all species. After noting the procedures of earlier workers and using only Pyrex in the source, a systematic variation of many parameters was made until 60% dissociation, with usually 99% of the atoms in the ground state, was obtained. This fortuitously high fraction was obtained with '99.5% pure' oxygen with the addition of about 3% molecular hydrogen and 1% water vapour. Once this dissociation fraction was obtained it was stable over several weeks. However, opening the system to air required a tedious search for the optimum conditions, which could take many days. The procedure was not quantifiable other than the maximum number of ground-state atoms usually did not correspond with maxima of either the atomic or molecular ions. Electron energy-loss spectra at various angles identified the atomic and molecular metastable states present in the target beam and discharge on/off cycles helped identify the fractions of such states in the beam. The main metastable states identified were $^1$D (1.96 eV), $^1$S (4.17 eV) of atomic oxygen and the a $^1\Delta_g$ (0.98 eV), b $^1\Sigma_g^+$ (1.64 eV) and A $^3\Sigma_u^+$ (4.48 eV) of molecular oxygen.

### *2.2. Calibration methods*

The elastically scattered electrons were unambiguously identified by the 127° energy analyser, their angular distributions were obtained by rotation of the analyser around the axis of the atomic beam and the elastic differential cross sections were calibrated by the method of relative gas flows described in detail by Williams and Willis (1975). The helium elastic cross section was the secondary standard value.

Total scattering cross sections were measured by a beam attenuation method described by Brackmann *et al* (1958) and Bederson and Kieffer (1971). The attenuation of the incident electron beam by a molecular oxygen beam relative to that of the same partially dissociated beam was measured. A constant mass flow of gas through the atomic source was maintained. Then the ratio of atomic to molecular cross sections, $Q_a$ and $Q_m$ respectively, is given by

$$Q_a/Q_m = [(S'/S) - 1 + D]/D\sqrt{2} \tag{1}$$

where $D$ is the molecular dissociation fraction, $S'$ and $S$ are the detected signals with the dissociated and non-dissociated beams. The dissociation fraction is measured by an RF mass filter and the molecular cross section measured using a non-dissociated beam. The basic method is essentially unchanged from that used in the earliest crossed-beams measurements; however, there are many important improvements. First, Brackmann *et al* used an AC detection scheme but the present work used gated scalers which permit identification of background signals and their minimisation. The limits of detection were consequently about $10^{-13}$ A and less than 1 count/s respectively. Secondly, the earlier work used the molecular oxygen total cross section of Bruche (1927) whereas the present molecular total cross section has been measured simultaneously with the atomic to molecular cross section ratio. Thirdly, in the work of Neynaber *et al* (1961) the angular resolution of the electron gun was 25°, defined as 'the scattering angle for which the efficiency of detection of scattering is 50%' in their apparatus. In the present work, using the same definition, the angular resolution is energy dependent but has about an average of 2° except at an energy of 0.5 eV when it is 4°. This resolution makes a significant difference to the measured attenuation ratio

as indicated from the present angular distribution measurements. Fourthly, in the experiment of Neynaber *et al* (1961), the need for the greatest possible beam intensity required the use of source pressures higher than those satisfying effusive flow conditions. Consequently it was necessary to make corrections for atom and molecule collisions near the source and for values of the ratio of atomic to molecular velocities different from the expected $\sqrt{2}$ factor. Their factor was −20% which was zero in the present work basically because the limit of detection of scattered electrons was about six orders of magnitude smaller which meant that lower source pressures could be used. Finally their experiment did not use energy analysis for either the incident or transmitted beam whereas the present work used energy analysis for all electron detectors and could readily distinguish between elastically and inelastically scattered electrons.

### *2.3. Phaseshift analysis*

The technique used to analyse the differential cross section data has been discussed in detail elsewhere (Allen 1986, Allen *et al* 1987, Allen and McCarthy 1987). Briefly, the approach is based on a rational scattering function of the form

$$S_l(\boldsymbol{a}) = \prod_{n=1}^{N} (\lambda^2 - \beta_n^2)/(\lambda^2 - \alpha_n^2) \tag{2}$$

where $\lambda = l + 0.5$ and $\boldsymbol{a} = \{a_n\}$ is the set of all the real and imaginary parts of the $2N$ complex parameters $a_n$, $b_n$. The parameters $\{a_n\}$ are determined by minimising

$$\chi^2 = (M - 2N)^{-1} \sum_{i=1}^{M} (\sigma_i - \sigma(\theta_i, \boldsymbol{a}))^2/(\Delta\sigma_i)^2 \tag{3}$$

where $\sigma_i$ is the measured value of the differential cross section at angle $\theta_i$ with statistical error $\Delta\sigma_i$ and $\sigma(\theta_i, \boldsymbol{a})$ is the parametrised value of the differential cross section. Provided that non-statistical errors are small enough, the value of $\chi^2$ should be close to one. One of the advantages of the above approach is that it allows us to vary the phaseshifts for a large number of relevant partial waves via a much smaller number of open parameters. In this case phaseshifts up to $l = 100$ (which ensured convergence) were optimised via four open parameters ($N = 2$). Furthermore a rigorous statistical error analysis is possible.

## 3. Results and discussion

### *3.1. Elastic scattering*

Measured values of the elastic differential cross sections at five energies between 8.7 and 0.54 eV are shown in figures 2 to 6. The general character of the differential cross sections is that as the energy is decreased, the cross section values become smaller and the angular distribution flatter. The angular minimum near 60° in the earlier measurements of Dehmel *et al* (1976) is not indicated in any of our measurements and is presumed to be of 'apparatus origin'. A detailed discussion of systematic uncertainties in measurement of elastic scattering on this apparatus was given by Williams and Willis (1975). In the present work all identified systematic errors summed to about the size of the data points in figure 3 and are discussed further below.

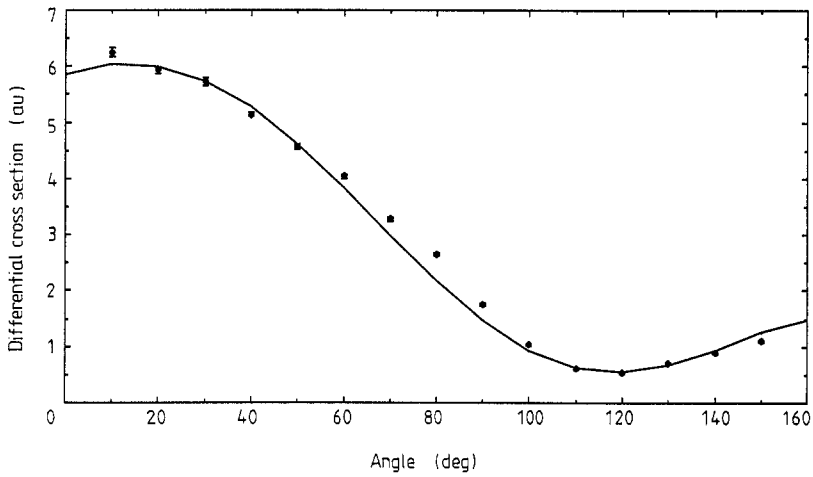


**Figure 2.** Absolute differential cross section for 8.7 eV electrons scattered elastically by atomic oxygen. The error bars represent statistical errors. The full curve is the fit to the data via the scattering function given by equation (2).

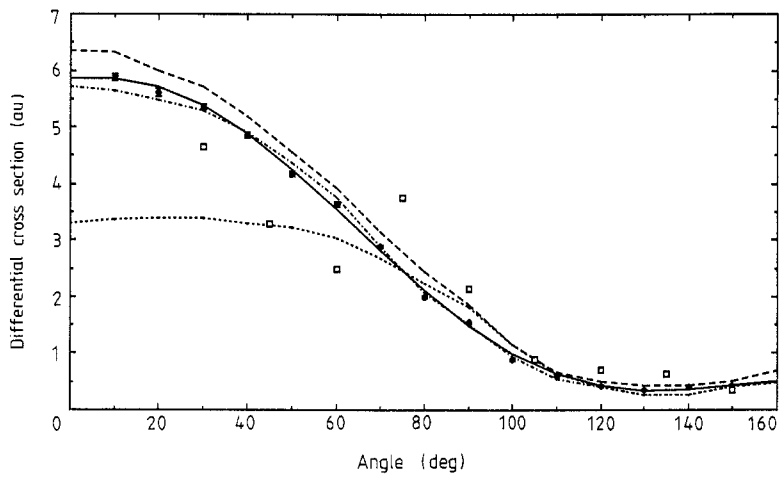


**Figure 3.** Absolute differential cross section for 4.9 eV electrons scattered elastically by atomic oxygen. The present data are shown by full squares with statistical uncertainty smaller than the size of the squares. The full curve is the fit to the data via the scattering function given by equation (2). The variational (BG) calculation of Nesbet (1977) is shown by the short broken (bottom) curve, the polarised pseudostate result of Tambe and Henry (1976) by the chain (middle) curve and the distorted-wave calculations of Blaha and Davis (1975) by the long broken (upper) curve. The measurements of Dehmel *et al* (1976) are shown by open squares.

At 4.9 eV there are three theoretical methods to compare with the measured values. The experimental uncertainty is sufficiently small that the distorted wave and Bethe-Goldstone results do not agree with the measured values at scattering angles less than 100°. The polarised pseudo-state method used by Tambe and Henry (1976) gives values in close agreement with the experiment. The Bethe-Goldstone method as used by Thomas and Nesbet (1975a, b) considerably underestimates the forward scattering

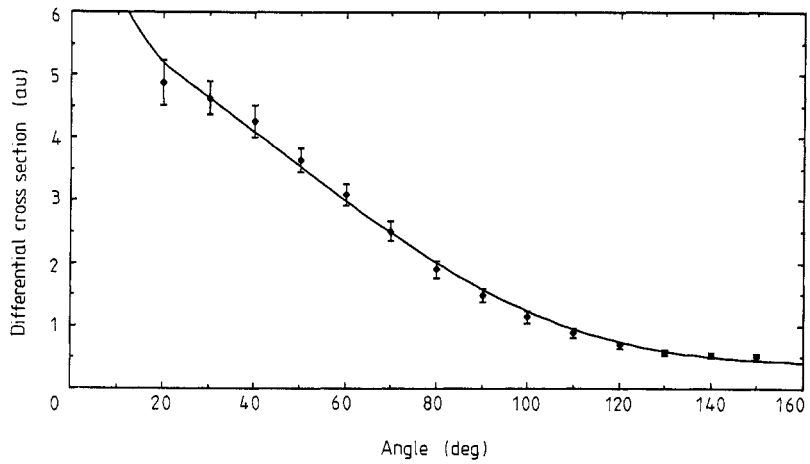


**Figure 4.** Absolute differential cross section for 3.4 eV electrons scattered elastically by atomic oxygen. The error bars represent statistical errors. The full curve is the fit to the data via the scattering function given by equation (2).

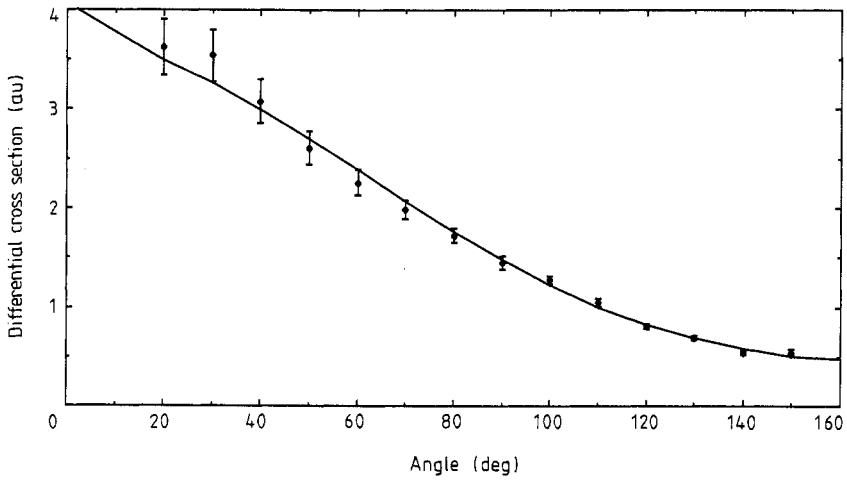


**Figure 5.** Absolute differential cross section for 2.18 eV electrons scattered elastically by atomic oxygen. The error bars represent statistical errors. The full curve is the fit to the data via the scattering function given by equation (2).

even though the full effects of long-range polarisation and short-range correlation were thought to be nearly completely taken into account. The distorted-wave model used by Blaha and Davis (1975) includes a polarisation potential which does not describe short-range correlation effects. The major difference between these theories is the amount of short-range correlation in the model.

The first few phaseshifts at each energy are given in table 1. The energy dependence of the phaseshifts for the $l = 0$, 1 and 2 partial waves is shown in figure 7. The phaseshifts show a smooth variation as a function of energy.

At 4.90 eV, the energy at which there is the greatest interface between theory and experiment, we have applied a 'smoothing procedure' to minimise the impact of non-statistical inconsistencies in the differential cross section data, as done previously

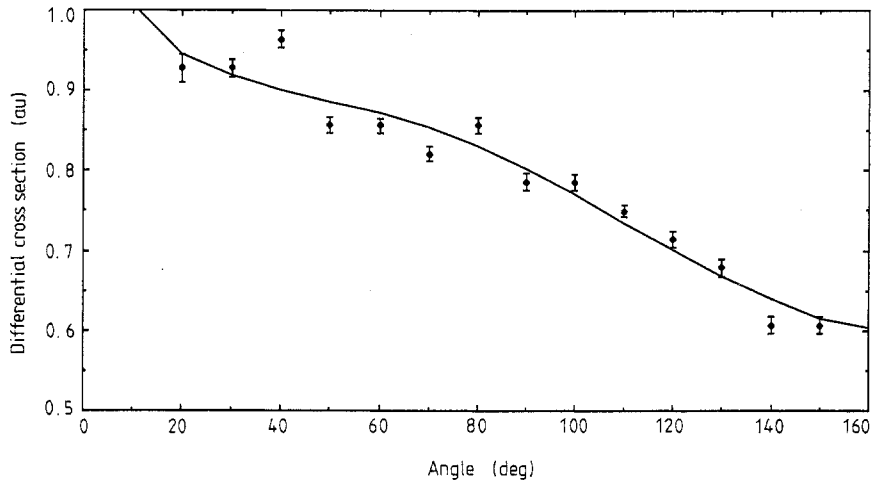


**Figure 6.** Absolute differential cross section for 0.54 eV electrons scattered elastically by atomic oxygen. The error bars represent statistical errors. The full curve is the fit to the data via the scattering function given by equation (2).

**Table 1.** The phaseshifts for elastic scattering of electrons from atomic oxygen determined by a least-squares minimisation fit. The experimental total elastic cross section, $\sigma_{int}^{exp}$, and momentum transfer cross section, $\sigma_{mt}^{exp}$, have been calculated from the experimental phaseshifts. The theoretical values are from Thomas and Nesbet (1975a, b).

| Energy (eV) | $k$ (au) | $\delta_0$ | $\delta_1$ | $\delta_2$ | $\delta_3$ | $\sigma_{int}^{exp}$ | $\sigma_{int}^{th}$ | $\sigma_{mt}^{exp}$ | $\sigma_{mt}^{th}$ |
|---|---|---|---|---|---|---|---|---|---|
| 8.71 | 0.8 | −1.18 | −0.49 | 0.04 | 0.008 | 29.9 | — | 18.3 | — |
| 4.90 | 0.6 | −0.79 | −0.30 | 0.01 | 0.002 | 26.7 | 23.2 | 14.4 | 14.1 |
| 3.40 | 0.5 | −0.69 | −0.18 | −0.01 | — | 25.2 | 20.7 | 15.1 | 13.4 |
| 2.18 | 0.4 | −0.51 | −0.09 | — | — | 20.8 | 18.1 | 14.1 | 12.7 |
| 0.54 | 0.2 | −0.18 | −0.01 | — | — | 9.9 | 10.8 | 9.1 | 10.1 |

for e-Na scattering (Allen *et al* 1987). This was achieved by allowing those points that made the largest contribution to the $\chi^2$ value to be shifted horizontally in steps of half a degree, having in mind the angular resolution of about 2° (and uncertainty in energy of about 0.25 eV) discussed previously. This improved the value of $\chi^2$ from 13.1 to 1.3. This allowed reasonable estimates of regularised statistical errors to be made on the phaseshifts. Details of the statistical regularisation are given by Allen and McCarthy (1987). The polarised pseudostate result of Tambe and Henry (1976) was the *a priori* information which was weighted such that the $\chi^2$ remained just less than two. The phaseshifts and errors obtained from this smoothed data are shown in table 2. It can be seen by comparison with table 1 that the smoothing procedure has not changed the values of the phaseshifts significantly.

Integral elastic and momentum transfer cross sections calculated from the phaseshifts (up to $l = 100$, to ensure convergence) are shown in table 1. The regularised values obtained from the smoothed data at 4.9 eV were $\sigma_{int}^{exp} = 26.7\ a_0^2$ with an error of 10% and $\sigma_{mt}^{exp} = 14.5\ a_0^2$ with an error of 5%. The smoothing procedure has not changed the median values of the cross sections significantly. The calculated values of the

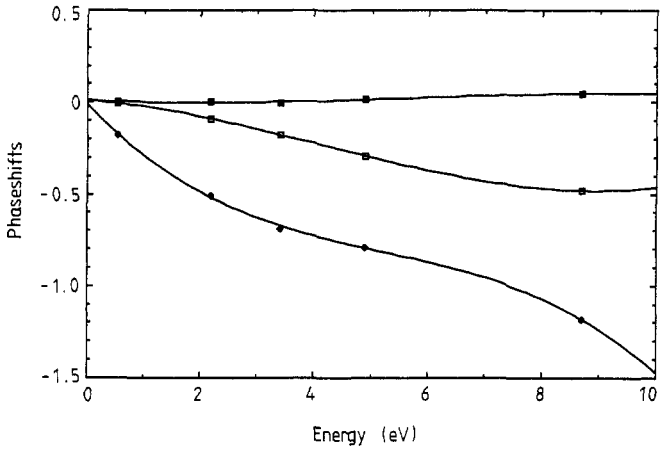


**Figure 7.** Phaseshifts as a function of energy. The $l = 0$ phaseshifts are indicated by the diamonds, $l = 1$ by the open squares and $l = 2$ by the dark squares. The full curves represent third-order polynomial fits to the phaseshifts for each partial wave.

**Table 2.** Phaseshifts obtained from the data at 4.9 eV, smoothed as described in the text, together with the associated statistical errors.

| $l$ | 0 | 1 | 2 | 3 | 4 |
|---|---|---|---|---|---|
| $\delta l$ | −0.79 | −0.30 | 0.015 | 0.0016 | −0.000 04 |
| $\Delta\delta l$ (%) | 1 | 1 | 5 | 17 | >100 |

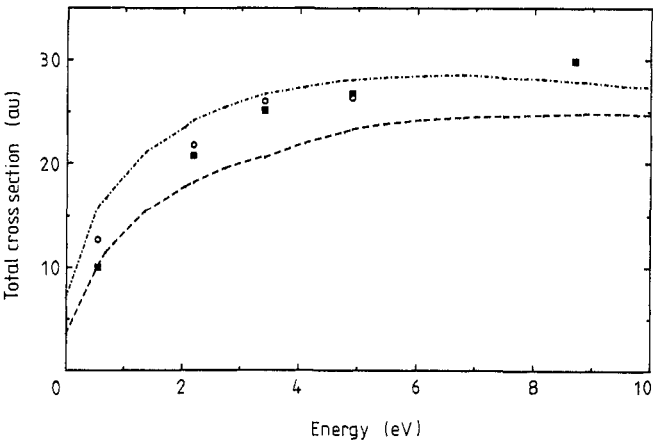


**Figure 8.** Total cross sections for scattering of electrons by atomic oxygen as a function of energy. The values determined from the phaseshift analysis are shown as full squares. The error bar at 4.9 eV is obtained as discussed in the text. The measured total cross sections are shown as open circles. The broken (lower) curve represents the BG results of Nesbet and the chain (upper) curve the polarised pseudostate calculations of Tambe and Henry.

integral cross sections in table 1 are compared with the BG and PS results in figure 8 and, unlike the differential cross section at 4.9 eV, do not discriminate conclusively between these two theoretical models.

At the energies of the present work the total scattering cross section is the sum of the integral elastic and inelastic cross sections, the latter are expected to be less than about 5% of the former for both atomic and molecular oxygen (see, for example, Thomas and Nesbet 1975a, b, Trajmar *et al* 1971). In atomic oxygen at 4.9 eV, Thomas and Nesbet predict integral elastic and inelastic ($^1$D and $^1$S) cross sections of 22.3 and 0.89 $a_0^2$ respectively. In molecular oxygen at 5 eV, Trajmar *et al* give the integral elastic and inelastic (electronic and vibrational) cross sections as 24.84 and 0.54 $a_0^2$ respectively. Consequently the present measured total cross sections at 5 eV may be considered as upper limits of the integral elastic cross section which value can be adjusted according to the value one wishes to assign to the integral inelastic cross section. Table 3 lists the measured total cross sections. The molecular oxygen values are close to those of Zecca *et al* (1986); the values of Griffiths *et al* (1982), Bruche (1927) and Salop and Nakano (1970) are lower, while those of Sunshine *et al* (1967), Shyn and Sharp (1982) and Dababneh *et al* (1988) are higher. The last mentioned authors discuss these data and theoretical values. Figure 8 indicates that these measured total cross sections are in good agreement with the values of the integral elastic cross sections calculated from the phaseshifts except at the lowest energy of 0.5 eV. The reason for this disagreement is not known but the most probable source of error would be the measured molecular contributions to the scattered signal.

**Table 3.** Total cross section values ($a_0^2$) in atomic and molecular oxygen. The numbers in brackets are the experimental uncertainties.

| Energy (eV) | 0.54 | 2.18 | 3.40 | 4.90 |
|---|---|---|---|---|
| Atomic oxygen | 12.7 (1.7) | 21.9 (1.9) | 26.1 (1.7) | 26.3 (1.9) |
| Molecular oxygen | 19.3 (0.9) | 25.5 (0.8) | 26.4 (0.7) | 26.8 (0.6) |

## Acknowledgments

We would like to thank Professor I E McCarthy for helpful discussions.

## References

Allen L J 1986 *Phys. Rev.* A **34** 2706-9
Allen L J, Brunger M J, McCarthy I E and Teubner P J O 1987 *J. Phys. B: At. Mol. Phys.* **20** 4861-8
Allen L J and McCarthy I E 1987 *Phys. Rev.* A **36** 2570-5
Bederson B and Kieffer L J 1971 *Rev. Mod. Phys.* **43** 601-40
Blaha M and Davis J 1975 *Phys. Rev.* A **12** 2319-24
Boyd R F L and Green G W 1958 *Proc. Phys. Soc.* **71** 351-6
Brackmann R T, Fite W L and Neynaber R H 1958 *Phys. Rev.* **112** 1157-61
Bruche 1927 *Ann. Phys., Lpz.* **83** 1065-73
Dababneh M S, Hziek Y F, Kwan C K, Smith S T, Stein T S and Uddin M N 1988 *Phys. Rev.* A **38** 1207-16
Daiber J W and Waldron H F 1966 *Phys. Rev.* **151** 51-5

Dehmel R C, Fineman M A and Miller D R 1974 *Phys. Rev.* A **9** 1564-8
—— 1976 *Phys. Rev.* A **13** 115-22
Griffiths T C, Charlton M, Clark G, Heyland G R and Wright G L 1982 *Positron Annihilation* (Amsterdam: North-Holland) pp 61-70
LeDourneuf M, Vo Ky Lan and Burke P G 1977 *Comment. At. Mol. Phys.* **7** 1-13
Lin S C and Kivel B 1959 *Phys. Rev.* **114** 1026-7
Neynaber R H, Marino L L, Rothe E W and Trujillo S M 1961 *Phys. Rev.* **123** 148-52
Nesbet R K 1977 *Comment. At. Mol. Phys.* **7** 15-22
—— 1980 *Variational Methods in Electron-Atom Scattering Theory* (New York: Plenum) pp 196-204
Salop A and Nakano H H 1970 *Phys. Rev.* A **2** 127-31
Seaton M J 1953 *Phil. Trans. R. Soc.* A **245** 469
Shyn T W and Sharp W E 1982 *Phys. Rev.* A **26** 1369-72
Sunshine G, Aubrey B B and Bederson B 1967 *Phys. Rev.* **154** 1-8
Tambe B R and Henry R J W 1976 *Phys. Rev.* A **14** 512-4
Temkin A 1957 *Phys. Rev.* **107** 1004-12
Thomas L D and Nesbet R K 1975a *Phys. Rev.* A **11** 170-3
—— 1975b *Phys. Rev.* A **12** 1729-30
Trajmar S, Cartwright D C and Williams W 1971 *Phys. Rev.* A **4** 1482-92
Williams J F 1988 *J. Phys. B: At. Mol. Opt. Phys.* **21** 2107-16
Williams J F and Willis B A 1975 *J. Phys. B: At. Mol. Phys.* **8** 1641-69
Zecca A, Brusa R S, Grisenti R, Oss S and Szmytkowski C 1986 *J. Phys. B: At. Mol. Phys.* **19** 3353-60